Interaction of 4-nitrothiophenol with low energy electrons: Implications for plasmon mediated reactions

Robin Schürmann (iD), Thomas F. M. Luxford (iD), Ivo S. Vinklárek, Jaroslav Kočišek (iD), Mateusz Zawadzki (iD), and Ilko Bald (iD)

View Online   Export Citation   CrossMark

Interaction of 4-nitrothiophenol with low energy electrons: Implications for plasmon mediated reactions

Robin Schürmann,[1,a] Thomas F. M. Luxford,[2] Ivo S. Vinklárek,[2] Jaroslav Kočišek,[2] Mateusz Zawadzki,[3] and Ilko Bald[1]

AFFILIATIONS

[1] Physical Chemistry, Institute of Chemistry, University of Potsdam, Karl-Liebknecht-Str. 24-25, 14476 Potsdam-Golm, Germany

[2] J. Heyrovský Institute of Physical Chemistry of the Czech Academy of Sciences, Dolejškova 3, 18223 Prague, Czech Republic

[3] Department of Atomic, Molecular and Optical Physics, Faculty of Applied Physics and Mathematics, Gdańsk University of Technology, ul. G. Narutowicza 11/12, 80-233 Gdańsk, Poland

[a] Author to whom correspondence should be addressed: robin.schuermann@uni-potsdam.de

ABSTRACT

The reduction of 4-nitrothiophenol (NTP) to 4-4'-dimercaptoazobenzene (DMAB) on laser illuminated noble metal nanoparticles is one of the most widely studied plasmon mediated reactions. The reaction is most likely triggered by a transfer of low energy electrons from the nanoparticle to the adsorbed molecules. Besides the formation of DMAB, dissociative side reactions of NTP have also been observed. Here, we present a crossed electron-molecular beam study of free electron attachment to isolated NTP in the gas-phase. Negative ion yields are recorded as a function of the electron energy, which helps to assess the accessibility of single electron reduction pathways after photon induced electron transfer from nanoparticles. The dominant process observed with isolated NTP is associative electron attachment leading to the formation of the parent anion of NTP. Dissociative electron attachment pathways could be revealed with much lower intensities, leading mainly to the loss of functional groups. The energy gained by one electron reduction of NTP may also enhance the desorption of NTP from nanoparticles. Our supporting experiments with small clusters, then, show that further reaction steps are necessary after electron attachment to produce DMAB on the surfaces.

Published under license by AIP Publishing. https://doi.org/10.1063/5.0018784

INTRODUCTION

Electron–hole pairs generated in the decay of localized surface plasmons in noble metal nanoparticles (NPs) enable various applications in solar energy conversion and chemical synthesis.[1,2] These so-called hot electrons with an energy of typically 0 eV–3 eV above the Fermi level[3] can be transferred into the initially unoccupied orbitals of adsorbed molecules and trigger reactions therein.[4–10] It is assumed that electrons are transferred by chemical induced damping, where the surface plasmon resonance decays non-radiatively by transferring an electron from the valence band of the NP into the unoccupied molecular orbitals of the adsorbed molecules.[11] In this process, the transfer-probability and final energy of the electrons depend significantly on the electronic structure at the metal–organic interface, which is strongly influenced by the interaction of the metal with the chemisorbed molecules.[12–14] The reduction of 4-nitrothiophenol (NTP) on the surface of gold and silver nanoparticles has been studied in detail with spectroscopic techniques and acts as a model reaction for plasmon mediated reactions.[15–26] Depending on the environment in which the reaction is conducted, NTP can be reduced to a different degree resulting in mainly two observed products, 4-4'-dimercaptoazobenzene (DMAB)[27] or the completely reduced 4-aminothiophenol (ATP).[28] Even though the reactions crucially depend on the temperature[16,29] and the chemical environment,[30,31] such as pH[32] and the presence of O$_2$[24,33] or halide ions,[25] it is widely assumed that the reaction

is initially triggered by a light induced electron transfer from the NPs to the NTP.[34] In this way, a transient negative ion is formed, whose properties can also be studied in detail by attachment of a free low energy electron to the respective molecule. In this context, an electron is understood to be of low energy when its kinetic energy is below the ionization threshold of the molecule. A transient negative ion is rather unstable and likely to decay either by detachment of the extra electron or by the cleavage of molecular bonds, resulting in the formation of a negative fragment ion and one or more neutral fragments.[35] However, as the transformation of NTP to DMAB or ATP requires the transfer of four or six electrons, respectively, an NTP⁻ ion needs to be formed in an initial step, having sufficient stability that it does not decay immediately but is able to initiate further subsequent chemical transformations.

In previous studies using surface enhanced Raman scattering (SERS), the initial reaction steps in the plasmon mediated reaction of NTP on a gold surface driven by a silver nanoparticle and in a gold/silver nanojunction were examined, and the rapid formation of a stable NTP⁻ anion was observed.[20,21,26] The initial formation of NTP⁻ is assumed to be the rate determining step since intermediate products are typically not observed in SERS measurements monitoring the reaction of NTP.[20] The electron induced reaction steps leading to the formation of DMAB, which are proposed on the basis of experimental observations,[20,21] are also in accordance with thermodynamic calculations of NTP on Ag and Au electrodes.[36] Nevertheless, at low surface coverages of NTP, when the formation of DMAB is inhibited due to the lack of neighboring NTP molecules, the cleavage of the nitro group has been observed, resulting in formation of bare thiophenol (TP) on the NP surface.[19] The electron induced reaction pathways of NTP on light illuminated metal surfaces, which have been observed so far, are summarized in Fig. 1(a). Moreover, with ongoing illumination time, a reduction in the signal intensity of NTP and its reaction products has been observed, which has been assigned to the thermal cleavage of

the Ag–S bond.[37] The initially formed anionic states of NTP represent the transition or intermediate states that determine the further pathway of the subsequent reaction. However, these anionic states involved in the different reaction pathways, leading either to the formation of a stable anion or to a dissociation of the molecule, have not yet been investigated. By irradiation with low energy electrons in combination with negative ion mass spectrometry, the negative ion resonances leading to the formation of certain reaction products can be monitored.[35] Nevertheless, this procedure is very challenging in the solid state because typically electron energies above 5 eV are required in order to desorb the reaction products from the surface to detect them. Hence, the reactions occurring at the relevant electron energy regime for plasmon mediated reactions (<2 eV) remain obscure in such experiments.[38,39] Using a crossed electron-molecular beam setup, the interaction of molecules and electrons can be studied in detail with a high energy resolution, and the negative ion resonances can be determined down to the energy of thermal electrons.[35,40] Even though the position and intensity of the negative ion resonances can differ in the gas-phase compared to systems in the condensed phase,[35] for the plasmon mediated reactions of 8-bromoadenine[41] it was previously possible to explain the reactions observed on nanoparticles upon excitation of their surface plasmon resonance with the anionic resonances determined in gas-phase measurements.[42]

RESULTS AND DISCUSSIONS

Within the present study, the interaction of NTP with low energy electrons has been studied in the gas-phase by electron molecule collisions, in order to obtain an in-depth understanding of the electron induced reactions of isolated NTP. Therefore, a beam of gas-phase NTP has been crossed with a beam of low energy electrons of defined energy between 0 eV and 15 eV to generate transient negative ions in a setup sketched in Fig. 1(b). In this way, the electrons
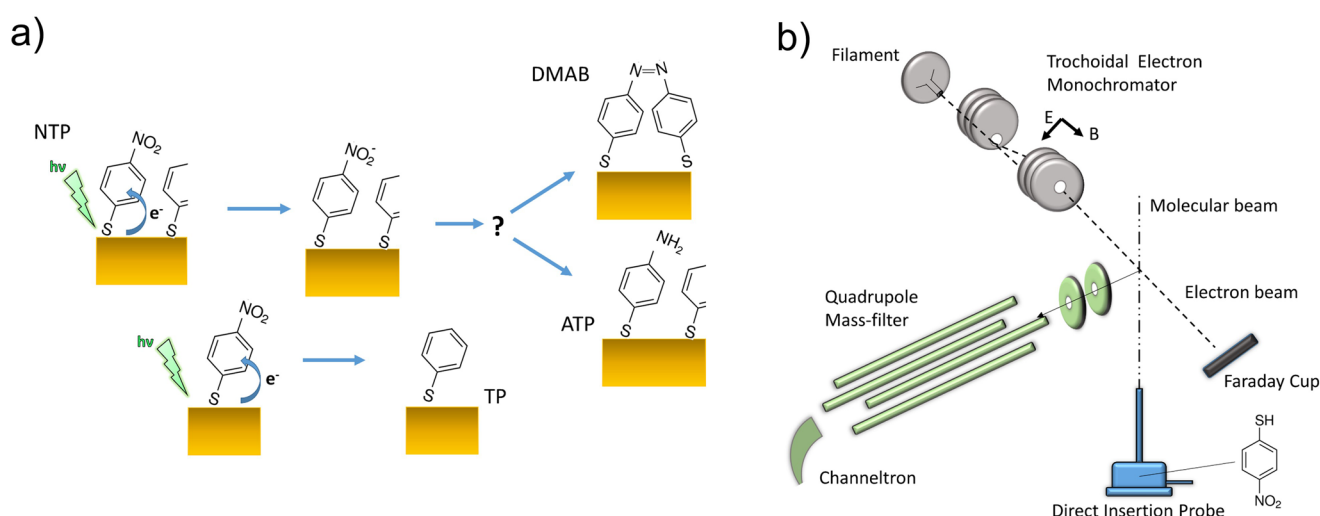

FIG. 1. (a) Scheme of the electron induced reaction pathways of NTP on a laser illuminated AuNP surface. (b) Schematic representation of the present experimental setup.

can temporally occupy a formerly empty molecular orbital of the NTP forming an anionic state, which can be either stable or decay by autodetachment of the extra electron or dissociation into an anion and one or more neutral fragments in a process called dissociative electron attachment (DEA),

$$NTP + e^- \rightarrow NTP^{-\#} \rightarrow anion\,(+\,neutral\,fragments).$$
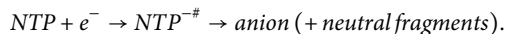
The resulting anions have been determined using negative ion mass spectrometry.

On the basis of the gas-phase electron molecule interactions, the reactions of NTP on a NP surface shall be interpreted, which are resulting from the plasmon mediated electron transfer from NPs to the adsorbed NTP. The electronic and vibrational modes of NTP might be significantly influenced by mixed metal molecular states of the metal–sulfide bond and resulting conformational changes, when the molecules are adsorbed on a surface, and consequently, this might cause an effect on the interaction of NTP with

low energy electrons compared to the gas-phase measurements.[43] More important multiple electron reduction happens on the surface in contrast to single collision conditions in the present experiment. Nevertheless, these experiments are a first step in obtaining a detailed understanding of the electron induced reactions of NTP.

In the gas-phase, eight different anions generated by electron attachment to NTP could be identified with a molecular mass of 32 u, 46 u, 92 u, 108 u, 124 u, 138 u, 154 u, and 155 u, respectively. For each observed anion, an energy spectrum has been recorded, where the anion yield is monitored as a function of the incident electron energy (see Fig. 2). Each fragment ion is formed within distinct resonant features, which reflect the initial resonant electron attachment process. Electrons having a specific energy are attached to NTP via a vertical Franck–Condon transition to form a specific transient negative ion state. Depending on the lifetime of the transient negative ion and the distribution of the electron over the molecule, effective dissociation reactions can occur. These reactions can proceed very
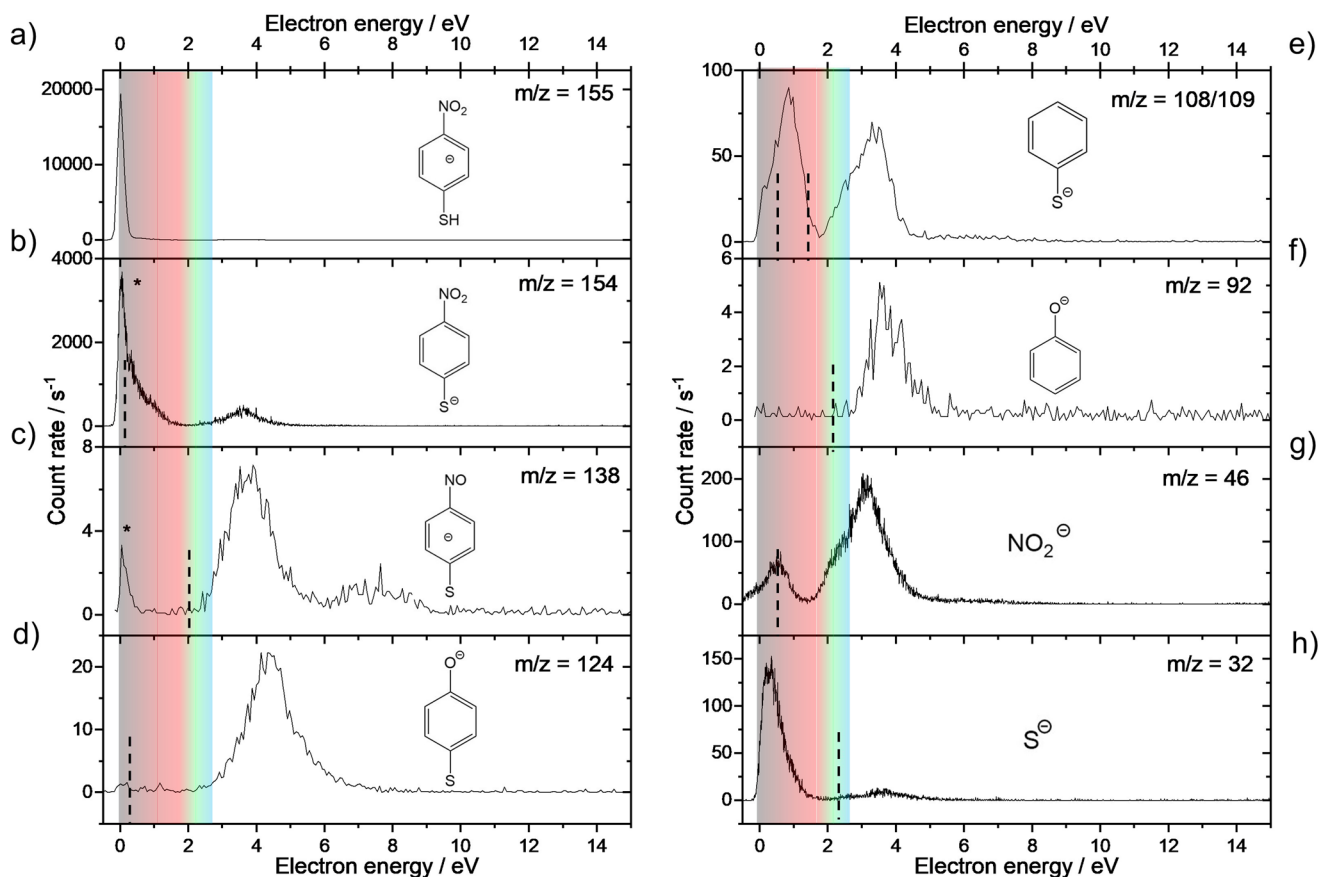

FIG. 2. Anion yield curves arising from low energy electron attachment shows the resonant formation of specific anionic fragments. The colored area marks the regime accessible for plasmonically generated electrons. Dashed lines in the spectrum show thermodynamic thresholds calculated at the B3LYP/aug-cc-pvtz level of theory in Gaussian16.[46] The peaks marked with * might arise due to possible artifacts in the measurement: the 0 eV signal in the 154 u spectrum might originate from the intensive resonance of NTP—due to the mass resolution of the quadrupole—whereas the 0 eV signal in the 138 u spectrum might be caused by residual contaminations in the collision chamber.

specifically with respect to both the bonds that are broken and the energy at which the electron attachment occurs.[44,45] The electron energies leading to the resonant formation of the respective anions from NTP are presented in Table I.

The anion with the highest yield is NTP⁻ at 155 u, which is formed in a single resonant signal peaking close to 0 eV. Based on previous studies of nitro-substituted benzenes, it can be assigned to a vibrational Feshbach resonance.[47] As the energy of the majority of the plasmonically generated electrons is slightly above the Fermi level, it is very likely that the transferred electrons from plasmonic NPs can form these resonances. The high yield and stability of NTP⁻ following the attachment of near 0 eV electrons explain well its rapid formation on laser illuminated plasmonic nanostructures.[20] Beyond that, DEA studies of other nitrophenol derivates in different cluster environments reveal a further stabilizing effect of the parent anion due to the environmental effects, which might occur in the plasmonic reactions of NTP as well.[40] The cross section of the anionic resonances on the surface can be highly enhanced compared to the gas-phase measurements due to coupling with image states.[48,49]

With a molecular mass of 154 u, the dehydrogenated parent anion (NTP–H)⁻ is observed with high yields within two resonant signals close to 0 eV with shoulders at 0.6 eV and at 3.6 eV. However, it is likely that the signal close to 0 eV is an artifact originating from NTP⁻ due to the low mass resolution of the used quadrupole mass filter. This is also confirmed by the calculated threshold of the reaction, which is 0.15 eV (see Fig. 3) So far, the formation of (NTP–H)⁻ has not been observed by SERS measurements of NTP reactions on NPs. On the one hand, the SERS spectrum of the dehydrogenated species is expected to be very similar to the respective NTP and NTP⁻ signals,[20] and on

the other hand, the dehydrogenation in the gas-phase experiments most likely originates from the thiol group mediated by a shape resonance.[50] In the case of NTP chemisorbed on the nanoparticle, hydrogen is replaced by the surface of the nanoparticle. The corresponding shape resonances may, therefore, induce desorption of NTP.

The anion at 138 u, formed by the loss of an oxygen atom from the nitro group and additional hydrogen, is observed from two resonances at 3.7 eV and 7.5 eV with a low yield in good agreement with the calculated threshold of the reaction of 2.02 eV (see Fig. 3). The energy of these two resonances is exceeding the energy of plasmonically generated electrons (colored region in Fig. 2), and the formation of (NTP–O)⁻ by the attachment of a single plasmonic electron is, therefore, unlikely. This is in good agreement with studies of plasmon induced reactions showing that (NTP–O)⁻ is formed following the attachment of two electrons.[20,21,36]

The anions at 109 u and 108 u are formed from two resonances at 0.9 eV and 3.4 eV and can be assigned to the cleavage of the nitro group from the phenyl ring, followed by hydrogen loss from sulfur in the case of 108 u. Unfortunately, we cannot separate contributions from these two channels in the present setup. These reaction channels match nicely the formation of thiophenol observed by Zhang *et al.* upon the illumination of AgNPs covered with a low density of NTP illuminated with 633 nm laser light.[19] The resonance at 0.9 eV is accessible for electrons generated under these conditions; however, the anion yield in this reaction channel is two orders of magnitude lower compared to the formation of NTP⁻. Hence, the cleavage of the nitro group can only be observed when the more probable formation of DMAB is hindered. The anionic counterpart with a mass of 46 u can be assigned to NO₂⁻. Both anions at

TABLE I. Energy and intensity of anions generated by electron attachment to NTP.

| m/z	Identity	Energy averaged intensity (relative to the parent ion)	Resonances in eV (peak intensity/s⁻¹) (sh indicates a shoulder peak)
32	S⁻	2.3 ± 1.1	0.4 (135.5) 3.7 (9.3)
46	NO₂⁻	7.4 ± 3.4	1.0 (61.7) 3.5 (185.9) 6.7 (5.1) sh
92	[NTP–SH–NO]⁻	0.2 ± 0.1	3.7 (4.1)
108 and 109	[NTP–NO₂–H]⁻ and [NTP–NO₂]	3.9 ± 1.8	0.9 (80.6) 3.4 (63.4) 6.1 (2.6) s
124	[NTP–NO–H]⁻	0.9 ± 0.4	4.4 (21.8)
138	[NTP–OH]⁻	0.3 ± 0.2	0.1 (3.0)–(may be background) 3.7 (6.5) 7.5 (1.4)
154	[NTP–H]⁻	47.7 ± 23.2	0.0 (3453)–(may be NTP⁻) 0.6 (867.2) sh 3.6 (362.9)
155	NTP⁻	100.0 ± 48.6	0.0 (18 414.1) 3.6 (488.2)
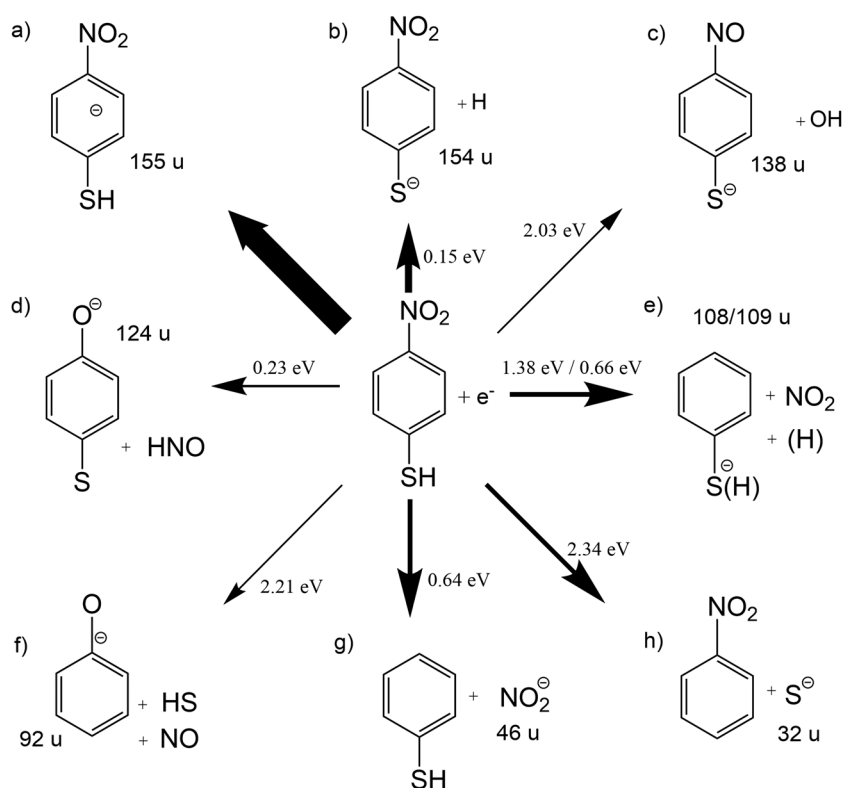
FIG. 3. Sketch of all observed reaction pathways. Values close to the arrows are calculated reaction thresholds assuming simple bond cleavages calculated at the B3LYP/aug-cc-pvtz level of theory in Gaussian16.[46] The thickness of the arrows reflects qualitatively the relative intensities of the reaction channels.

108 u/109 u and at 46 u are formed through resonances located at 1.0 eV and 3.5 eV, but with a different intensity ratio. NO_2^- is formed with three times higher intensity through the resonance at 3.5 eV than at 1.0 eV, whereas the 108/109 u signal appears with slightly higher intensity at 1.0 eV than at 3.5 eV despite much lower electron affinity of the $(NTP–NO_2)$ 109 u anion. The signals may be explained on the basis of calculated energetic thresholds of the reactions (see Fig. 3). While the threshold for the direct bond cleavage with charge remaining on the ring (109 u) is 1.54 eV, formation of the phenylthiol-radical anion (108 u) requires only 0.66 eV. Therefore, the 0.9 eV resonance enhancement is the contribution of the 108 u signal.

Ions observed at 124 u and 92 u are specific by the fact that they are formed after the removal of nitric oxide from the nitro group. Such a reaction needs a significant rearrangement within the molecule because a CN bond is replaced with a CO bond. Despite its complexity, it is a common reaction channel after electron attachment to nitro-substituted compounds.[40,51] The fragment anion with a mass of 124 u is formed by the loss of NO from the nitro group and hydrogen from sulfur through a single resonant feature with a maximum at 4.4 eV well above the energetic threshold of the reaction of only 0.3 eV (see Fig. 3). This difference may be explained by additional energy required for the rearrangement of the nitro group forming a barrier for the observed process. The fragment ion at 92 u originates from the cleavage of nitric oxide and the thiol group and is formed from a single resonance at 3.7 eV with a low yield. Energetic threshold for this process leading to

NO and HS formation is 2.2 eV. None of the resonances leading to NO loss is accessible via single electron transfer from plasmonic nanostructures.

Finally, a mass of 32 u S^- is formed through a strong resonance at only 0.4 eV and a very weak resonance at 3.7 eV. The second resonance can be explained by sulfur anion release after hydrogen migration to the phenyl ring, which requires an energy input of 2.34 eV. However, the low energy resonance cannot occur in the direct dissociation process. The present experiment, however, does not allow for unambiguous identification of the process. Sulfur represents a bridge to the nanoparticle surface, and therefore, the formation of S^- may contribute to desorption of molecules. Several mechanisms are assumed to describe the desorption of molecules from illuminated plasmonic surfaces: the molecules can desorb due to elevated temperatures[52] or electronic transitions[53,54] breaking the metal–molecule bond (i.e., the Au–S bond in the case of thiolated AuNPs). The present experiments suggest an additional desorption of NTP, and its reaction products from the NP surface[37] might be possible by cleaving the C–S bond. Our study shows that one electron reduction, which can be achieved in a single photon process, provides sufficient energy to break down the C–S bonds of NTP. The C–S bond strength may be comparable to the binding to the surface,[55] and desorption via the C–S cleavage channel may become important. Nevertheless, since on the one hand the bond-type and bond-strength of thiolated molecules on a heterogeneous metal surface are still under debate[56] and on the other hand the hybridized metal–molecular bonds might significantly alter the

TABLE II. Adiabatic electron affinities (AEAs) of NTP^- and its selected dissociation products calculated at the B3LYP/aug-cc-pvtz level of theory in Gaussian16.[46] Values in parentheses are from the NIST database.

Anion	Formula	AEA (eV)
NTP^-	$C_6H_4NO_2SH^-$	1.44
$(NTP–H)^-$	$C_6H_4NO_2S^-$	3.5
$(NTP–NO)^-$	$C_6H_4OSH^-$	2.35
$(NTP–NOH)^-$	$C_6H_4OS^-$	3.63
$(NTP–NO_2H)^-$	$C_6H_4S^-$	2.28 [2.345]
$NTP–NO_2$	C_4H_4SH	1.35
NO_2^-	NO_2^-	2.25 [2.2730]
S^-	S^-	2.21 [2.07]

electronic structure and reactivity of the C–S bond,[57] further evidence is required to validate whether the C–S bond cleavage is a reaction channel of NTP on a surface as well, as indicated by the gas-phase measurements.

Both fragmentation and desorption of the molecules may be enhanced by electrons due to the formation of anions. The reason is the energy gain due to electron affinity of the formed anions. Therefore, we are additionally listing the adiabatic electron affinities (AEAs), which were discussed in the text in Table II. The calculated values represent the situation of isolated NTP in the vacuum, which may be, however, altered when it is adsorbed on a metal surface.

In order to study the electron induced reactions of NTP dimers in the gas-phase, electron attachment to NTP dimers in He clusters has been performed, comparable to experiments described previously by Kočišek *et al.*[40] Within these measurements, beside the stable dimer anion with a mass of 310 u, only two further anions with a mass higher than 155 u have been observed at 172 u and 279 u. The latter might be a combination of an intact NTP with a mass of 155 u and the 124 u fragment and is likely to be in higher energetic resonances. Due to the possible loss of a nitrogen atom, this reaction channel will not be involved in the formation of DMAB. The results for NTP clusters indicate that the direct pathway from NTP oligomers to DMAB via single electron reduction is not possible. It will rather be the NTP^- parent anion that will be further reduced or interact with other available reactants on the NP surface to produce DMAB.

CONCLUSION

The yield curves of all anionic reaction products arising from electron attachment to gas-phase NTP have been determined, revealing a predominant formation of NTP^- compared to dissociative reaction pathways. NTP^- is favorably formed by electrons with an energy close to 0 eV, which corresponds to the typical energy of plasmonically generated electrons in noble metal NPs.[8] All observed dissociative reaction channels are leaving the phenyl ring intact and cleaving functional groups or parts of it. The most intense and, hence, the most relevant dissociative reaction channels are hydrogen abstraction, the loss of the nitro group, and the formation of S^-. All further fragments have been formed with a comparably low yield.

The DEA resonances are typically located at 0 eV, 1 eV, and 3.5 eV, and the first two are basically accessible in the light induced electron transfer from plasmonic nanoparticles. All anionic products, which are expected from SERS measurements, namely, the parent anion and the fragments arising from the cleavage of the C–N and the C–S bonds have been observed. The electron induced desorption might act as an alternative reaction pathway to the thermal desorption of the molecule from the NP surface, explaining the signal decrease in NTP and its reaction products in SERS measurements with ongoing illumination time. Further alternative reaction routes such as the cleavage of oxygen and nitric oxide from the nitro group have been observed as well, however, with some orders of magnitude of lower yield and at higher energies, indicating a minor role of this reaction pathway in the plasmon induced reaction of NTP. The present electron attachment experiments are supporting the existing models of the initial steps of electron induced reactions of NTP on NPs. However, single electron reduction is not sufficient for explaining the DMAB formation on NPs, as revealed in our experiments with small NTP_n clusters.

EXPERIMENTAL DETAILS

Chemicals: NTP with a purity of 96% was purchased from Alfa Aesar and used without further purification.

Negative ion mass spectrometry: The gas-phase molecular electron collision experiments have been performed using an experimental setup initially built by Stepanović *et al.*,[58] which has been modified toward measurements of low volatile compounds.[59] The electron beam is generated by using a trochoidal electron monochromator, providing electrons with an energy resolution of approximately 100 meV and a current of around 3 nA. The molecular beam is produced by subliming a solid NTP sample in a glass reservoir at a temperature of 40 °C, which is connected to a 1 cm long molybdenum capillary with an inside diameter of 0.5 mm. The reservoir is a part of the direct insertion probe inlet that enables exchange of solid samples without venting the main chamber of the setup. The electron and molecular beams are crossed under vacuum at a pressure of 1×10^{-6} mbar, and the generated anions are extracted from the interaction regions toward a quadrupole mass filter and detected subsequently with a channeltron detector. The electron energy was calibrated by the 4.4 eV resonance in the O^- yield from CO_2.[60]

SUPPLEMENTARY MATERIAL

See the supplementary material for the negative ion mass spectrum of NTP_n recorded under cluster conditions.

DATA AVAILABILITY

The data that support the findings of this study are available from the corresponding author upon reasonable request.

REFERENCES

[1] S. Linic, P. Christopher, and D. B. Ingram, Nat. Mater. **10**, 911 (2011).

[2] S. Linic, U. Aslam, C. Boerigter, and M. Morabito, Nat. Mater. **14**, 567 (2015).

[3] A. Manjavacas, J. G. Liu, V. Kulkarni, and P. Nordlander, ACS Nano **8**, 7630 (2014).

[4] G. V. Hartland, L. V. Besteiro, P. Johns, and A. O. Govorov, ACS Energy Lett. **2**, 1641 (2017).

[5] P. Christopher and M. Moskovits, Annu. Rev. Phys. Chem. **68**, 379 (2017).

[6] M. L. Brongersma, N. J. Halas, and P. Nordlander, Nat. Nanotechnol. **10**, 25 (2015).

[7] M. J. Kale, T. Avanesian, and P. Christopher, ACS Catal. **4**, 116 (2014).

[8] S. Mukherjee, F. Libisch, N. Large, O. Neumann, L. V. Brown, J. Cheng, J. B. Lassiter, E. A. Carter, P. Nordlander, and N. J. Halas, Nano Lett. **13**, 240 (2013).

[9] J. Szczerbiński, L. Gyr, J. Kaeslin, and R. Zenobi, Nano Lett. **18**, 6740 (2018).

[10] J. Szczerbiński, J. B. Metternich, G. Goubert, and R. Zenobi, Small **16**, e1905197 (2020).

[11] B. Foerster, A. Joplin, K. Kaefer, S. Celiksoy, S. Link, and C. Sönnichsen, ACS Nano **11**, 2886 (2017).

[12] A. J. Therrien, M. J. Kale, L. Yuan, C. Zhang, N. J. Halas, and P. Christopher, Faraday Discuss. **214**, 59 (2019).

[13] B. Foerster, V. A. Spata, E. A. Carter, C. Sönnichsen, and S. Link, Sci. Adv. **5**, eaav0704 (2019).

[14] M. J. Seo, G. W. Kim, P. V. Tsalu, S. W. Moon, and J. W. Ha, Nanoscale Horiz. **5**, 345 (2020).

[15] R. Schürmann, K. Ebel, C. Nicolas, A. R. Milosavljević, and I. Bald, J. Phys. Chem. Lett. **10**, 3153 (2019).

[16] R. M. Sarhan, W. Koopman, R. Schuetz, T. Schmid, F. Liebig, J. Koetz, and M. Bargheer, Sci. Rep. **9**, 3060 (2019).

[17] X. Ren, E. Cao, W. Lin, Y. Song, W. Liang, and J. Wang, RSC Adv. **7**, 31189 (2017).

[18] D. A. Nelson and Z. D. Schultz, J. Phys. Chem. C **122**, 8581 (2018).

[19] Z. Zhang, T. Deckert-Gaudig, P. Singh, and V. Deckert, Chem. Commun. **51**, 3069 (2015).

[20] H.-K. Choi, K. S. Lee, H.-H. Shin, and Z. H. Kim, J. Phys. Chem. Lett. **7**, 4099 (2016).

[21] H.-K. Choi, W.-H. Park, C.-G. Park, H.-H. Shin, K. S. Lee, and Z. H. Kim, J. Am. Chem. Soc. **138**, 4673 (2016).

[22] K. Kim, J.-Y. Choi, and K. S. Shin, J. Phys. Chem. C **119**, 5187 (2015).

[23] E. M. van Schrojenstein Lantman, P. de Peinder, A. J. G. Mank, and B. M. Weckhuysen, ChemPhysChem **16**, 489 (2015).

[24] S. Sheng, X. Ji, X. Yan, H. Wei, Y. Luo, and H. Xu, J. Phys. Chem. C **124**, 11586 (2020).

[25] L. Qiu, G. A. Pang, G. Zheng, D. Bauer, K. Wieland, and C. Haisch, ACS Appl. Mater. Interfaces **12**, 21133 (2020).

[26] C.-F. Wang, B. T. O'Callahan, D. Kurouski, A. Krayev, and P. Z. El-Khoury, J. Phys. Chem. Lett. **11**, 3809 (2020).

[27] B. Dong, Y. Fang, L. Xia, H. Xu, and M. Sun, J. Raman Spectrosc. **42**, 1205 (2011).

[28] W. Xie and S. Schlücker, Nat. Commun. **6**, 7570 (2015).

[29] A. A. Golubev, B. N. Khlebtsov, R. D. Rodriguez, Y. Chen, and D. R. T. Zahn, J. Phys. Chem. C **122**, 5657 (2018).

[30] C. Ma, Y. Liu, J. Wang, S. Wu, Q. Zhang, P. Song, and L. Xia, J. Raman Spectrosc. **49**, 1395 (2018).

[31] Q. Zhang, Y. Zhou, X. Fu, E. Villarreal, L. Sun, S. Zou, and H. Wang, J. Phys. Chem. C **123**, 26695 (2019).

[32] M. Sun, Y. Huang, L. Xia, X. Chen, and H. Xu, J. Phys. Chem. C **115**, 9629 (2011).

[33] X. Yan, L. Wang, X. Tan, B. Tian, and J. Zhang, Sci. Rep. **6**, 30193 (2016).

[34] E. L. Keller and R. R. Frontiera, ACS Nano **12**, 5848 (2018).

[35] I. Bald, J. Langer, P. Tegeder, and O. Ingólfsson, Int. J. Mass Spectrom. **277**, 4 (2008).

[36] L.-B. Zhao, J.-L. Chen, M. Zhang, D.-Y. Wu, and Z.-Q. Tian, J. Phys. Chem. C **119**, 4949 (2015).

[37] M. A. Mahmoud, Phys. Chem. Chem. Phys. **19**, 32016 (2017).

[38] C. Olsen and P. A. Rowntree, J. Chem. Phys. **108**, 3750 (1998).

[39] P. Rowntree, L. Sanche, L. Parenteau, M. Meinke, F. Weik, and E. Illenberger, J. Chem. Phys. **101**, 4248 (1994).

[40] J. Kočišek, K. Grygoryeva, J. Lengyel, M. Fárník, and J. Fedor, Eur. Phys. J. D **70**, 98 (2016).

[41] R. Schürmann and I. Bald, Nanoscale **9**, 1951 (2017).

[42] R. Schürmann, K. Tanzer, I. Dąbkowska, S. Denifl, and I. Bald, J. Phys. Chem. B **121**, 5730 (2017).

[43] S. K. Saikin, R. Olivares-Amaya, D. Rappoport, M. Stopa, and A. Aspuru-Guzik, Phys. Chem. Chem. Phys. **11**, 9401 (2009).

[44] I. Bald, I. Dąbkowska, E. Illenberger, and O. Ingólfsson, Phys. Chem. Chem. Phys. **9**, 2983 (2007).

[45] H. Abdoul-Carime, I. Bald, E. Illenberger, and J. Kopyra, J. Phys. Chem. C **122**, 24137 (2018).

[46] M. J. Frisch, G. W. Trucks, H. B. Schlegel, G. E. Scuseria, M. A. Robb, J. R. Cheeseman, G. Scalmani, V. Barone, G. A. Petersson, H. Nakatsuji, X. Li, M. Caricato, A. V. Marenich, J. Bloino, B. G. Janesko, R. Gomperts, B. Mennucci, H. P. Hratchian, J. V. Ortiz, A. F. Izmaylov, J. L. Sonnenberg, D. Williams-Young, F. Ding, F. Lipparini, F. Egidi, J. Goings, B. Peng, A. Petrone, T. Henderson, D. Ranasinghe, V. G. Zakrzewski, J. Gao, N. Rega, G. Zheng, W. Liang, M. Hada, M. Ehara, K. Toyota, R. Fukuda, J. Hasegawa, M. Ishida, T. Nakajima, Y. Honda, O. Kitao, H. Nakai, T. Vreven, K. Throssell, J. A. Montgomery, Jr., J. E. Peralta, F. Ogliaro, M. J. Bearpark, J. J. Heyd, E. N. Brothers, K. N. Kudin, V. N. Staroverov, T. A. Keith, R. Kobayashi, J. Normand, K. Raghavachari, A. P. Rendell, J. C. Burant, S. S. Iyengar, J. Tomasi, M. Cossi, J. M. Millam, M. Klene, C. Adamo, R. Cammi, J. W. Ochterski, R. L. Martin, K. Morokuma, O. Farkas, J. B. Foresman, and D. J. Fox, Gaussian 16, Revision C.01, 2016.

[47] J. P. Johnson, D. L. McCorkle, L. G. Christophorou, and J. G. Carter, J. Chem. Soc., Faraday Trans. Part 2 **71**, 1742 (1975).

[48] I. I. Fabrikant, Phys. Rev. A **76**, 012902 (2007).

[49] K. Nagesha and L. Sanche, Phys. Rev. Lett. **81**, 5892 (1998).

[50] B. C. Ibănescu and M. Allan, J. Phys.: Conf. Ser. **194**, 012030 (2009).

[51] N. L. Asfandiarov, S. A. Pshenichnyuk, V. G. Lukin, I. A. Pshenichnyuk, A. Modelli, and Š. Matejčik, Int. J. Mass Spectrom. **264**, 22 (2007).

[52] A. Turchanin, M. El-Desawy, and A. Gölzhäuser, Appl. Phys. Lett. **90**, 053102 (2007).

[53] P. Avouris and R. E. Walkup, Annu. Rev. Phys. Chem. **40**, 173 (1989).

[54] M. Bonn, S. Funk, C. Hess, D. N. Denzler, C. Stampfl, M. Scheffler, M. Wolf, and G. Ertl, Science **285**, 1042 (1999).

[55] D. L. Kokkin, R. Zhang, T. C. Steimle, I. A. Wyse, B. W. Pearlman, and T. D. Varberg, J. Phys. Chem. A **119**, 11659 (2015).

[56] M. S. Inkpen, Z. F. Liu, H. Li, L. M. Campos, J. B. Neaton, and L. Venkataraman, Nat. Chem. **11**, 351 (2019).

[57] M. Sakamoto, K. Hyeon-Deuk, D. Eguchi, I.-Y. Chang, D. Tanaka, H. Tahara, A. Furube, Y. Minagawa, Y. Majima, Y. Kanemitsu, and T. Teranishi, J. Phys. Chem. C **123**, 25877 (2019).

[58] M. Stepanović, Y. Pariat, and M. Allan, J. Chem. Phys. **110**, 11376 (1999).

[59] J. Langer, M. Zawadzki, M. Fárník, J. Pinkas, J. Fedor, and J. Kočišek, Eur. Phys. J. D **72**, 112 (2018).

[60] R. Dressler and M. Allan, Chem. Phys. **92**, 449 (1985).